Selective Excitation of Low Frequency Drift Waves by Density Modulation and Parametric Excitation of Higher Frequency Mode

Subir Biswas, Debjyoti Basu,* Rabindranath Pal,† and Nikhil Chakrabarti
Saha Institute of Nuclear Physics, 1/AF Bidhannagar, Kolkata 700064, India
(Received 31 May 2013; published 13 September 2013)

Excitation of low frequency drift waves in a radial region of a weak density gradient is demonstrated experimentally by strong temporal modulation of the plasma density. Though a parallel electron current can destabilize drift waves throughout the region, we observe mode selection at the resonant location matching the frequency of modulation. Parametric mode-mode interaction among two excited drift modes to destabilize a higher frequency one is reported under the specific condition of the growth rate. Theoretically estimated growth rates fit well with the experiment.

DOI: 10.1103/PhysRevLett.111.115004 PACS numbers: 52.35.Kt, 52.35.Ra

Drift wave fluctuations in magnetized plasma arise because of a spatially inhomogeneous density (n_0) perpendicular to a steady magnetic field (B). It is generally believed that the low frequency drift wave is the primary candidate behind anomalous particle transports across the confining magnetic field line [1–3] in tokamaks and other fusion devices. The dynamics of drift modes has been extensively studied [4–6], and still remains one of the major topics of interest due to some unresolved issues. Its characteristics and stability analysis have been studied in a series of experiments [7–14] in various laboratories in different parameter regimes. In most of these experiments the wave is either spontaneously excited due to collisions of electrons with ions and neutrals or excited by driving an electron current parallel to the magnetic field or by $\mathbf{E} \times \mathbf{B}$ rotation [12,15]. The mode is excited in the region of the strongest density gradient where a constant drift frequency ω_* $(= k_\theta v_d,\ v_d = T_e/eBL_n)$, can be assumed. Here $k_\theta (= m/r)$ is the poloidal wave number, m is the poloidal mode number, v_d is the diamagnetic velocity, L_n is the density scale length and T_e is the electron temperature. However, in the central region of the plasma, the density gradient is generally low and varies slowly with radius and so is the drift frequency. Note here that the observation of such low frequency peaks for drift wave turbulence spectra in plasmas was reported before [16], but remains unattended.

In this Letter, we report in detail the selective excitation of a low frequency drift mode in the MaPLE (Magnetized Plasma Linear Experimental) device [17]. In the region there exists a parallel flow of electrons causing the drift modes to have a strong growth rate over a band of frequencies. However, the frequency selection for excitation is done in the experiment by driving a strong modulation of electron density with a frequency that is resonant in this region. To the best of our knowledge, this is an excitation scenario that has not been reported so far. The parallel velocity component of the excited $m = 2$ mode couples nonlinearly with the externally created density fluctuation to produce a parallel current fluctuation with twice the frequency. This selectively drives a second drift mode resonant in a nearby location. In this experiment the $m = 4$ drift mode is stable and hence not excited. Interestingly, this mode starts appearing as the modulation parameters cross a threshold value to drive parametric mode-mode coupling in the plasma. The excited mode satisfies the frequency and wave number matching conditions. A parametric mode-mode coupling of drift waves was reported before [18] where the pump drift mode excites two lower frequency modes which are normally stable. In contrast, we demonstrate that the pump drift wave can parametrically excite the higher frequency drift mode with a substantial growth rate of the lower frequency mode.

In our experiment with the MaPLE [17] device, 0.30 m in diameter and 2.40 m in length, plasma is produced by the ECR discharge method [19,20] in a magnetic field of about 875 G by launching a 2.45 GHz microwave through a rectangular wave guide from one end. Nitrogen is used as the filling gas. Various Langmuir probes are inserted from radial ports for determining the electron density n_e, temperature T_e, and floating potential as a function of radius. The radial profiles of n_e, T_e and plasma potential (obtained from the observed floating potential and adding T_e correction) with a filling pressure of $p = 3.8 \times 10^{-5}$ torr are shown in Fig. 1. In the discharge, where T_e is about 4–5 eV, N^+ is the dominant ion species as N_2^+ is comparatively short lived. Ion temperature T_i, is also measured using a retarded field energy analyzer and found in the range of 0.2–0.6 eV depending on the filling gas pressure. A 0.5 m spectrometer with a photomultiplier tube measures the line integrated optical emission along the diameter to monitor the fluctuations in electron density.

The density fluctuations ($\tilde{n}/n_0 \sim 40\%$) are created by modulating microwave power with a frequency of 300 Hz naturally available from the microwave generator. Microwave power is monitored from a directional coupler at its output end. Figures 2(a) and 2(b) show fluctuating parts of the microwave power and n_e (obtained from ion saturation current) near the axis. The corresponding power

 © 2013 American Physical Society

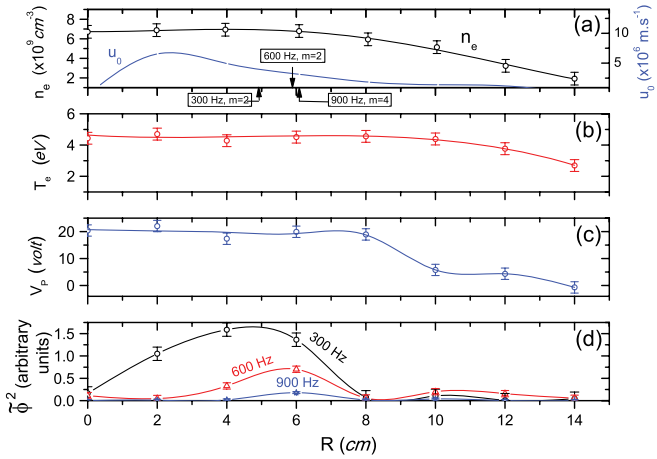

FIG. 1 (color online). Radial profile of (a) the plasma density (n_e) and parallel electron velocity (u_0), (b) electron temperature (T_e), (c) plasma potential (V_P), and (d) $\tilde{\phi}^2$ for 300 Hz, 600 Hz and 900 Hz frequency at $p = 3.8 \times 10^{-5}$ torr.

spectra [Figs. 2(e) and 2(f)] show a large peak at 300 Hz, but negligible contributions at other frequencies. To find out the response of the density fluctuation on the plasma we monitored the floating potential near the axis and light intensity [Figs. 2(c) and 2(d)]. The power spectrum of the potential fluctuation [Fig. 2(g)] shows hardly any power at frequencies other than 300 Hz. However, the total light intensity, which is related to the diameter averaged electron density, shows [Fig. 2(h)] a significant amount of power at 600 Hz ($\sim 7\%$ of that at 300 Hz). This clearly indicates the presence of strong density fluctuations at this frequency at radii away from the center.

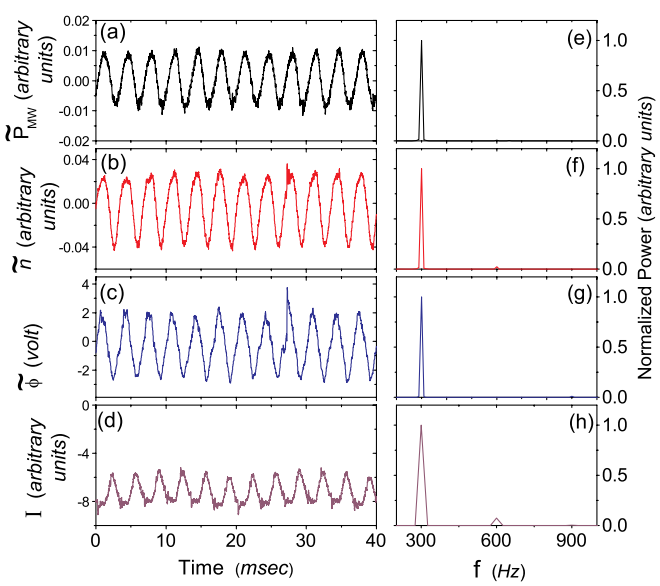

FIG. 2 (color online). Temporal fluctuations of (a) microwave power, $\tilde{P}_{\mathrm{MW}}$, (b) plasma density, $\tilde{n}$, (c) floating potential, $\tilde{\phi}$, and (d) total light intensity, I. (e)–(h): the corresponding frequency spectra. $\tilde{n}$ and $\tilde{\phi}$ are at $R = 1$ cm. $p = 3.8 \times 10^{-5}$ torr.

We obtained detailed radial variation of the floating potential fluctuations ($\tilde{\phi}$) with a 2-probe radial array to cause minimum disturbances to the plasma. Figure 3 shows the time series signals of $\tilde{\phi}$ along with their power spectra at different radii varying from 2 cm to 8 cm at $p = 3.8 \times 10^{-5}$ torr. The spectra are obtained by fast Fourier transform of the time series records of 10 000 points at a sample interval of 4 microseconds. The spectra clearly show the presence of 300 Hz and 600 Hz frequencies over a radial region and have strength much above the turbulence level. We feel these low frequency peaks might have been what was previously observed for drift wave turbulence in cylindrical plasmas [13,16] and probably originated from the region of weaker density gradient. In our experiment, $\tilde{\phi}$ for these frequencies peak within the $R = 4$–6 cm region [see Fig. 1(d)]; more specifically, for 300 Hz the maximum power is at about $R = 5$ cm whereas it peaks slightly outwards at around $R = 6$ cm for 600 Hz. In addition, we observe a distinct 900 Hz frequency component in the signal having substantial strength and peaking around $R = 6$ cm.

To verify that these fluctuations are waves propagating in the azimuthal direction we deployed two sets of Langmuir probes: probe set 1 consisting of three floating probes (FP0, FP90, FP180) each inserted radially at three azimuthal locations 90 degrees apart; and probe set 2, having two floating probes (FP1, FP2) inserted radially and separated in azimuthal direction (distance between them 5 mm). The mode numbers are obtained from them at the above frequencies. In doing so we first filtered the raw signals in a narrow band around the corresponding frequencies. Figures 4(a)–4(c) show the signals at 300 Hz, 600 Hz, and 900 Hz, respectively, from the probe set 1. The figures clearly show the evidence of wave propagation in the azimuthal direction, more specifically, in the electron

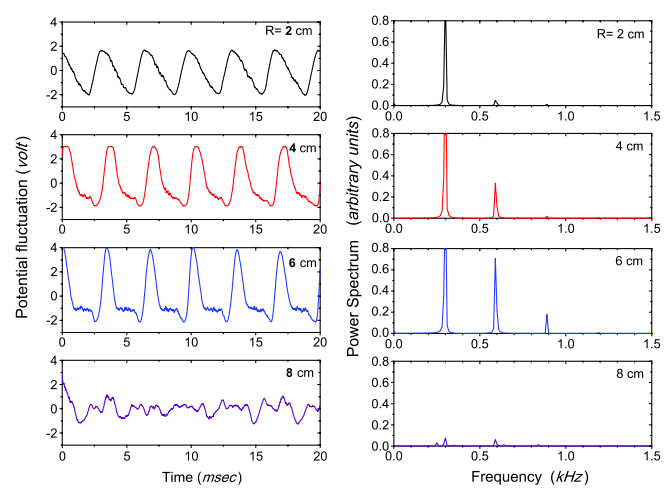

FIG. 3 (color online). The time series of floating potential fluctuations and the corresponding power spectra at different radial positions. $p = 3.8 \times 10^{-5}$ torr.

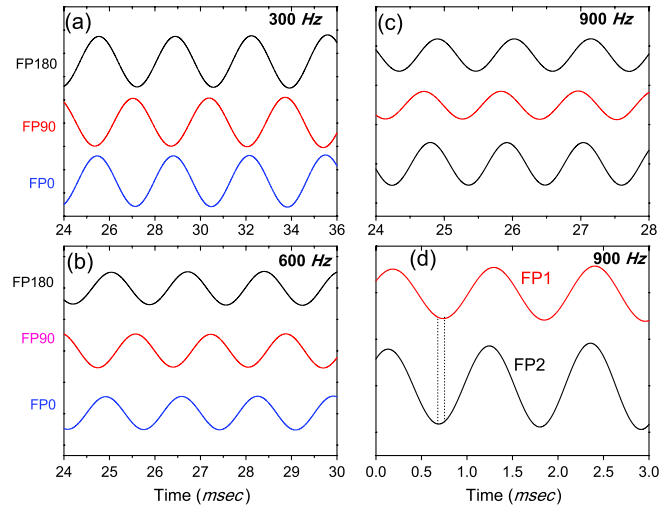

FIG. 4 (color online). Potential fluctuations at (a) 300 Hz, (b) 600 Hz, (c) 900 Hz with probe set 1 [FP0, FP90, FP180], placed 90° apart azimuthally], and (d) 900 Hz with probe set 2 [FP1, FP2] placed 5 mm apart poloidally.

diamagnetic drift direction, having a mode number $m = 2$ for the 300 and 600 Hz frequencies. The signals from the two probes of the probe set 2 confirm this observation independently and give a phase velocity of 1.3×10^4 cm/s for 600 Hz. Interestingly, the 900 Hz signals from the probe set 1 show almost no phase difference suggesting it is either $m = 0$ or $m = 4$ mode. However, the signals from the probe set 2 remove this ambiguity showing a phase difference of about 20 degrees [Figure 4(d)] that corresponds to $m = 4$ mode.

It is worth noting from Fig. 1 that the 300, 600, and 900 Hz fluctuation peaks occur in the region where plasma density decreases slowly with almost no electric field. The density falls sharply beyond $R = 8$ cm after decreasing slowly in the 4–8 cm region. In the former region the fluctuation spectra do not show any observable peak. A local minimum appears in the $R = 8$–10 cm region where the plasma potential has a sharp gradient. This minimum presumably occurs due to the suppression of low frequency modes by the $\mathbf{E} \times \mathbf{B}$ rotational shear. The average electric field E in this region is ~7.25 volt/cm. This may give rise to Kelvin-Helmholtz instability [21,22], though the estimated frequency $(1/4\pi\Delta)(E/B)$ is much higher, ~65 kHz [Δ(~1 cm) is the scale length of the shear layer].

The ECR produced plasma of the MaPLE device has a parallel flow of electrons in the $R = 2$ to 6 cm region [1(a)]. This is confirmed by measuring the velocity distribution function with the retarded field energy analyzer placing its collector facing parallel and antiparallel to the magnetic field in succession. At $p = 3.8 \times 10^{-5}$ torr the flowing electrons have about 40 eV of energy.

As the parallel electron current can destabilize drift modes, so it is quite likely that the azimuthally propagating waves at 300 and 600 Hz frequencies are excited drift frequencies selected resonantly as a consequence of strong density fluctuation ($\tilde{n}/n_0 \sim 40\%$) at 300 Hz. This is possible only if the plasma condition is suitable for considerable growth rate [23]. To look into this possibility we examine the dispersion relation for drift waves obtained from the standard drift wave model for density and vorticity fluctuations having a radial electron density gradient and a parallel electron current [24,25]:

$$\frac{d}{dt}\left(\frac{\tilde{n}}{n_0} + \ln n_0\right) = \frac{1}{n_0 e}[\nabla_\parallel J_\parallel + \nabla_\parallel J_{\parallel\mathrm{ext}}] \tag{1}$$

$$\frac{d}{dt}\left(\frac{1}{B\omega_{ci}}\nabla_\perp^2\varphi - \frac{\tilde{n}}{n_0} - \ln n_0\right) = -\frac{\nu_i}{B\omega_{ci}}\nabla_\perp^2\varphi \tag{2}$$

where $d/dt \equiv \partial/\partial t + [(\hat{e}_z \times \nabla\varphi)/B]\cdot\nabla$, $J_\parallel = (T_e/m_e\nu_e)\nabla_\parallel(\tilde{n}/n_0 - e\varphi/T_e)$, $J_{\parallel\mathrm{ext}} = -e\tilde{n}u_0$, u_0 is the parallel electron flow velocity, ω_{ci} is the ion cyclotron frequency, and ν_e, ν_i are the collision frequencies of the electron and ion, respectively. In the above $J_\parallel$ and $J_{\parallel\mathrm{ext}}$ are the driving terms for destabilizing the wave whereas the ion collisions stabilize it. For comparison with experimental results the real frequency and growth rate in our weakly ionized low β plasma can be obtained in local approximation [10]:

$$\Omega = \frac{\omega_*}{(1+b)}, \qquad \Gamma = \frac{\omega_*}{\nu_\parallel(1+b)}\left(\frac{b\omega_*}{(1+b)^2} + k_\parallel u_0\right) - \frac{b\nu_i}{(1+b)}. \tag{3}$$

Here the terms $k_\parallel$, $k_\perp$ are the parallel and perpendicular wave vectors. The wave dispersive effect is denoted by $b = k_\perp^2\rho_s^2$, where the ion-acoustic gyroradius $\rho_s = c_s/\omega_{ci}$, ion acoustic speed $c_s = \sqrt{T_e/m_i}$, m_e, m_i are the electron and ion masses, and $\nu_\parallel = k_\parallel^2 T_e/m_e\nu_e$. In our experiment the first term in Eq. (3) is negligible compared to the ion collision term. So only external current in the form of flowing electrons in the MaPLE device can destabilize the drift modes.

In the reported experiments of drift wave excitations, the modes are observed with a frequency corresponding to the strong gradient region. However, the scenario is different here. As we observe the excited modes in the region $R = 4$–8 cm, where no strong density gradient developed. So, the length scale is fairly large there. On the other hand, Fig. 1 reveals axial electron flow in this region. We estimate point-to-point drift frequencies corresponding to $m = 2$ from Eq. (3) which are obtained by local approximation though it is well known that drift modes have a radial extent in cylindrical geometry. The positions of the observed modes corresponding to 300, 600, and 900 Hz are indicated by arrows in the Fig. 1(a). The resonance positions corresponding to the drift frequencies of 300 and 600 Hz match well with the observed peaks of these fluctuations. So it seems the imposed density oscillation at 300 Hz

resonantly selects the radial location for the drift wave excitation if the growth rate is favorable. In Fig. 5 we plot the growth rate Γ for different mode numbers at the relevant frequencies obtained from Eq. (3) using the parameters of our experimental condition: $n_e = 7 \times 10^9\,\mathrm{cm}^{-3}$, $T_e = 4$ eV, $T_i = 0.2$-0.3 eV, $u_0 = 3.75 \times 10^6$ m/sec, $k_\parallel = 1.8\,\mathrm{m}^{-1}$, $\nu_e = 4.64 \times 10^5$/sec, and $\nu_i = 2.3 \times 10^4$/sec.

A growth rate of 300 Hz, $m = 2$ mode is reasonably high. So the strong externally imposed 300 Hz density oscillations seem to excite this drift mode by resonance frequency selection at the proper radial location. But it is not clear why the $m = 1$ mode at this frequency is not excited. It could be that the effect caused by rectangular wave guide antenna radiation is causing preferential selection of the $m = 2$ mode. This excited mode couples nonlinearly with the strong density fluctuation created externally to produce a second harmonic fluctuation. Thus clearly, the parallel current has a 600 Hz, $m = 2$ component given by $\sim \sin(1200\pi t - 2\theta)$ and it seems responsible for driving the 600 Hz drift mode whose resonance point lies in the near vicinity and has a large growth rate as seen in Fig. 5.

No electron flow is observed at the higher filling pressure of $p = 3.8 \times 10^{-4}$ torr which explains why no drift mode at 600 Hz is seen at the higher pressure even if strong density modulation at 300 Hz is present.

However, the observation of the 900 Hz peak with $m = 4$ mode at the nearby position is not readily explainable because Fig. 5 suggests this mode has a negative growth rate and hence should be damped. One possibility is that this mode $(\omega_1, \boldsymbol{k}_1)$ is excited because of nonlinear interaction, more specifically, its parametric coupling [18,26,27] with the 600 Hz mode that acts as the pump wave $(\omega_0, \boldsymbol{k}_0)$. The lower frequency 300 Hz $(\omega_2, \boldsymbol{k}_2)$ mode in the plasma is the balancing third mode in the plasma. Both the frequency as well as wave number matching conditions, namely, $\omega_1 = \omega_0 + \omega_2$ and $\boldsymbol{k}_1 = \boldsymbol{k}_0 + \boldsymbol{k}_2$, are satisfied, supporting this proposition. To confirm it further the strength of parametric coupling can be estimated from the following standard expression [27]:

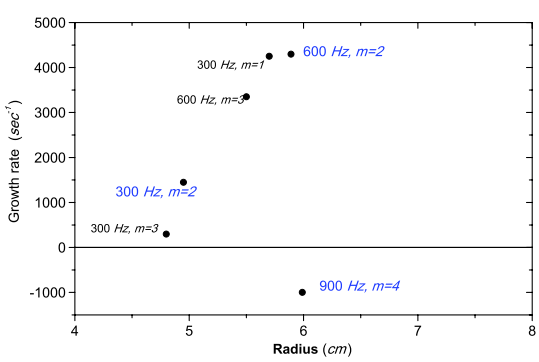

FIG. 5 (color online). Linear growth rates and radial positions for different azimuthal mode numbers m in the experimental condition with $p = 3.8 \times 10^{-5}$ torr.

$$\epsilon^L(\omega_1, \boldsymbol{k}_1) - \frac{\varphi_0^2 |M|^2}{\epsilon^L(\omega_2, \boldsymbol{k}_2)} = 0. \tag{4}$$

Here $\epsilon^L(\omega_1, \boldsymbol{k}_1)$, $\epsilon^L(\omega_2, \boldsymbol{k}_2)$ are the linear dielectric functions for the excited and the low frequency plasma modes, respectively, φ_0 is the dimensionless amplitude of the pump mode, and M is a dimensionless matrix element representing the coupling between the pump mode and excited mode. Expressing $\epsilon^L(\omega_1, \boldsymbol{k}_1)$ by its resonance approximation relation [18] as

$$\epsilon^L(\omega_1, \boldsymbol{k}_1) \approx \frac{k_D^2}{k^2}\left\{\frac{\omega_1 - (\Omega_1 + i\Gamma_1)}{\Gamma_1}\right\} \tag{5}$$

and similarly for $\epsilon^L(\omega_2, \boldsymbol{k}_2)$, from Eq. (4) we get the parametric growth rate for the excited mode $(\omega_1 \approx \Omega_1 + i\gamma)$ as

$$\gamma = (\Gamma_1\Gamma_2 + A^2\Omega_1\Omega_2)/(\Gamma_1 + \Gamma_2) \tag{6}$$

where $A^2 = \varphi_0^2 |M|^2 k_1^2 k_2^2 / k_D^4$ and $k_D = 2\pi/\lambda_D$. When we examine Eq. (6) we observe that if both the modes Ω_1, Ω_2 are stable in the plasma, i.e., their linear growth rates in absence of parametric coupling $\Gamma_1, \Gamma_2 < 0$, then there is a threshold for the parametric excitation of $(\Omega_1, \boldsymbol{k}_1)$ only if Ω_2 is negative. This means $\Omega_1 = \omega_0 - |\Omega_2|$, that is the pump wave decays into two lower frequency waves. This is what is normally observed in parametric decay [27]. On the other hand, if both Ω_1 and Ω_2 are positive satisfying $\Omega_1 = \omega_0 + \Omega_2$ and the modes are stable, then $\gamma < 0$ and no parametric excitation is possible. However, if $\Gamma_1 < 0$ whereas $\Gamma_2 > 0$, that is the low frequency mode Ω_2 is a growing mode but the high frequency mode Ω_1 is a stable one, then the later is parametrically excited by the pump wave when $|\Gamma_2| > |\Gamma_1|$, i.e., the normal growth rate of the lower frequency mode in more than the decay rate of the higher frequency mode. Here a threshold value of the pump amplitude, φ_{0M} arises as $k_1 k_2 |M| \varphi_{0M} / k_D^2 = \sqrt{|\Gamma_1||\Gamma_2|/\Omega_1\Omega_2}$. In our experiment, $\Omega_1/2\pi = 900$ Hz and $\Omega_2/2\pi = 300$ Hz and from Fig. 5 we observe that the growth rate of the 300 Hz, $m = 2$ mode is more than the decay rate of the 900 Hz, $m = 4$ mode, satisfying the criteria. So the 900 Hz mode that we observed in our experiment is parametrically coupled and excited by the 600 Hz, $m = 2$ mode. In the experiment the value of the normalized coupling coefficient, as given by $k_1 k_2 |M| / k_D^2 = \sqrt{|\Gamma_1||\Gamma_2|/\Omega_1\Omega_2}/\varphi_0$, comes out to be 1.04 which confirms significant strong coupling for parametric excitation. To determine the threshold value φ_{0M} experimentally we observed that we can vary the amplitude of the pumping wave at 600 Hz by changing the filling pressure. The result obtained is depicted in Fig. 6, which clearly reveals the existence of a threshold value of the pump wave amplitude.

In conclusion, we demonstrated mode-selective excitation of a low frequency drift wave in the weak density gradient region by strong temporal modulation of the plasma density at a frequency resonant with the mode in this region. The parallel velocity induced due to the excited mode couples with the imposed density modulation to

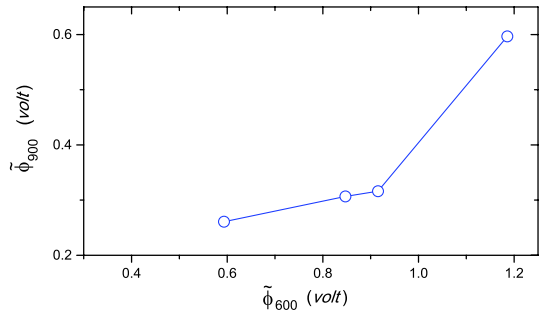

FIG. 6 (color online). Variation of potential amplitude, $\tilde{\phi}_{900}$ of the parametrically excited mode at 900 Hz with potential amplitude, $\tilde{\phi}_{600}$ of the pump wave at 600 Hz.

produce the spatiotemporal current modulation at the second harmonic frequency that also causes mode-selective excitation of drift mode in the nearby region. We also observe that under the condition of a sufficient growth rate for the lower frequency mode, the two modes cause parametric excitation of a higher frequency drift mode that is otherwise stable in the plasma.

The authors would like to thank Mr. M. Chattopadhyay, Mr. S. Basu, and Mr. D. Das for technical assistance. This work is supported by the Department of Atomic Energy, Government of India.

*Present address: Instituto de Ciencias Nucleares-UNAM, Mexico D.F., 04510, Mexico
†rabindranath.pal@saha.ac.in

[1] B. B. Kadomtsev, Nucl. Fusion **31**, 1301 (1991).
[2] N. Brenning, R. L. Merlino, D. Lundin, M. A. Raadu, and U. Helmersson, Phys. Rev. Lett. **103**, 225003 (2009).
[3] B. A. Carreras, IEEE Trans. Plasma Sci. **25**, 1281 (1997).
[4] W. Horton, Rev. Mod. Phys. **71**, 735 (1999).
[5] G. R. Tynan, A. Fujisawa, and G. McKee, Plasma Phys. Controlled Fusion **51**, 113001 (2009).
[6] R. Hatakeyama, C. Moon, S. Tamura, and T. Kaneko, Contrib. Plasma Phys. **51**, 537 (2011).
[7] H. W. Hendel, B. Coppi, F. Perkins, and P. A. Politzer, Phys. Rev. Lett. **18**, 439 (1967).
[8] T. K. Chu, B. Coppi, H. W. Hendel, and F. W. Perkins, Phys. Fluids **12**, 203 (1969).
[9] P. A. Politzer, Phys. Fluids **14**, 2410 (1971).
[10] R. F. Ellis, E. Marden-Marshall, and R. Majeski, Plasmas Phys. **22**, 113 (1980).
[11] E. Agrimson, N. D'Angelo, and R. L. Merlino, Phys. Rev. Lett. **86**, 5282 (2001).
[12] E. Marden-Marshall, R. F. Ellis, and J. E. Walsh, Plasma Phys. Controlled Fusion **28**, 1461 (1986).
[13] T. Klinger, A. Latten, A. Piel, G. Bonhomme, T. Pierre, and T. D. de Wit, Phys. Rev. Lett. **79**, 3913 (1997).
[14] O. G. Christiane Schroder and T. Klinger, Phys. Plasmas **12**, 042103 (2005).
[15] P. Beyer, S. Benkadda, X. Garbet, and P. H. Diamond, Phys. Rev. Lett. **85**, 4892 (2000).
[16] H. L. Pecseli, T. Mikkelsen, and S. Larsen, Plasma Phys. **25**, 1173 (1983).
[17] R. Pal, S. Biswas, S. Basu, M. Chattopadhyay, D. Basu, and M. Chaudhury, Rev. Sci. Instrum. **81**, 073507 (2010).
[18] A. Y. Wong, M. V. Goldman, F. Hai, and R. Rowberg, Phys. Rev. Lett. **21**, 518 (1968).
[19] R. Geller, *Electron Cyclotron Resonance, Ion Source and ECR Plasmas* (IOP Publishing, London, 1996).
[20] E. S. Aydil, J. A. Gregus, and R. A. Gottscho, J. Vac. Sci. Technol. A **11**, 2883 (1993).
[21] T. Huld, A. Nielsen, H. L. Pecseli, and J. Rasmussen, Phys. Fluids B **3**, 1609 (1991).
[22] G. I. Kent, N. C. Jen, and F. F. Chen, Phys. Fluids **12**, 2140 (1969).
[23] O. E. Garcia, V. Naulin, A. H. Nielsen, and J. J. Rasmussen, Phys. Rev. Lett. **92**, 165003 (2004).
[24] A. Hasegawa and M. Wakatani, Phys. Rev. Lett. **50**, 682 (1983).
[25] T. S. Pedersen, P. K. Michelsen, and J. J. Rasmussen, Plasma Phys. Controlled Fusion **38**, 2143 (1996).
[26] T. K. Chu, H. W. Hendel, and T. C. Simonen, Phys. Fluids **16**, 2034 (1973).
[27] G. Weyl and M. Goldman, Phys. Fluids **12**, 1097 (1969).